Macromolecules

Article

pubs.acs.org/Macromolecules

Core-Liquid-Induced Transition from Coaxial Electrospray to Electrospinning of Low-Viscosity Poly(lactide-*co*-glycolide) Sheath Solution

C. J. Luo*,[†,‡] and M. Edirisinghe[‡]

[†]Department of Materials Science and Metallurgy, University of Cambridge, 27 Charles Babbage Road, Cambridge CB3 0FS, U.K.

[‡]Department of Mechanical Engineering, University College London, Torrington Place, London WC1E 7JE, U.K.

Supporting Information

ABSTRACT: Co-electrospinning has demonstrated that polymer solutions below the entanglement concentration can be made into fibers as an encapsulated core in an electrospinnable sheath solution containing a carrier/template polymer. The carrier polymer may require removal at a later stage. This work shows for the first time that without increasing the polymer concentration/molecular weight or needing a template polymer, simply infusing a liquid in the core nozzle can cause the sheath polymer solution (viscosity <20 mPa s) to electrospin instead of electrospray in a coaxial electrified jet. Different from coelectrospinning, the core liquid can be a common solvent such as water and does not require a readily electrospinnable carrier polymer. The process was not limited to one core liquid system; infusing solvents and nonsolvents with different properties in the core generated either beaded fibers or continuous fibers from the sheath solution. The process of fiber formation instead of particle breakup was attributed to the relaxation time of the elastic polymer sheath solution becoming longer than the growth rate of the Rayleigh instability in the compound jet upon the infusion of a second solvent in the core. Key parameters of the process included high surface tension of the core liquid (e.g., water and glycerol), high interfacial tension between the core and the sheath liquids, and electrohydrodynamic operating parameters such as flow rate and applied voltage. Given that charge was transferred from the sheath solution to the core liquid, differences in the dielectric constant and electrical conductivity of the core liquids showed little influence on the process. Fibers also formed irrespective of the miscibility and solubility of the solvent, though in the case of a nonsolvent, a lower miscibility was desirable to minimize polymer precipitation at the core−sheath interface. The process was investigated using poly(lactide-*co*-glycolide) as a model system, with polycaprolactone and polymethylsilsesquioxane systems presented as two additional examples. This work documents new roles of solvents in coaxial electrohydrodynamic processes and presents a useful method to obtain micro- and nanofibers from low-viscosity solutions without using a template polymer.

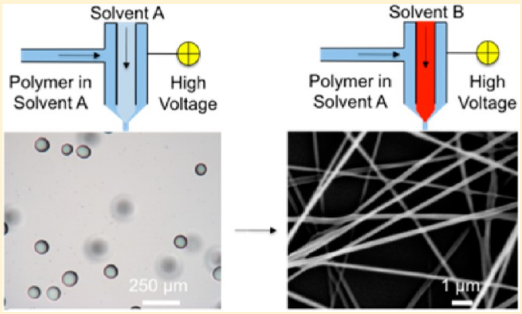

1. INTRODUCTION

Polymeric particles and fibers of micro- and nanometer diameters, with solid, porous, core−shell, or hollow configurations, have a wide range of important applications including drug delivery, tissue engineering, food sciences, sensors, filtration, acoustics, and energy harvesting.[1−5] A range of technologies have been studied to generate such products with specific properties, among which electrospray and electrospinning have gained widespread popularity over the past two decades for their simple apparatus design and versatile ability to process organic and inorganic materials.[1]

Both processes are kindred electrohydrodynamic (EHD) techniques, governed by electromechanical and hydrodynamic principles.[1] During an EHD process, a strong electric field (kilovolt range) is applied to a liquid infused through a capillary nozzle. The liquid forms a droplet at the capillary exit and becomes charged. Energy is supplied to deform the droplet. Taylor[6] showed the deformation of the droplet as a balance between the electrostatic stresses and the surface tension of the liquid. The deforming droplet remains motionless until the strength of the electric field reaches a critical value, at which the droplet assumes a conical shape (Taylor cone) and issues a fine, charged jet at the apex of the cone, reducing in size from milli/centimeter to nano/micrometer diameters. The jet remains steady if the mass and charge supplied to the jet are in balance to those issued from the Taylor cone.[7] The steady state of a jet continuously issued from a cone-shape droplet is called the cone-jet mode. Such a mode occurs within several coupled ranges of flow rates and voltages.[8] The cone-jet mode is the most desirable state during EHD processes, as near-monodisperse structures can be achieved.[9,10]

Received: August 13, 2014
Revised: October 29, 2014
Published: November 12, 2014

The jet issuing from a Taylor cone experiences a range of competing instabilities, including the surface tension driven Rayleigh–Plateau instability, and the electrically driven axisymmetric conducting instability and whipping/bending instability.[11,12] Depending on the viscoelasticity of the polymer solution, the dominating instability leads to either electrospray or electrospinning.[13,14] For electrospray, Rayleigh–Plateau instability dominates the process and manifests varicose waves on the surface of an EHD jet. The jet breaks up to form highly charged fine particles/beads, dispersed in a radial fashion due to Coulomb repulsion.[15] On the other hand, electrospray transits to electrospinning, when the viscoelasticity of the polymer solution partially or completely suppresses Rayleigh–Plateau instability, resulting in necklace-like beaded fibers or long continuous fibers.[11,16]

A versatile technology, EHD processes can form particles, capsules, bubbles, and fibers from a broad range of liquids.[4,17−20] Core–sheath configuration of the particles and fibers can be achieved by changing the single capillary nozzle to a coaxial or multiaxial nozzle (two or multiple nozzles in a concentric assembly), allowing the formation of a charged compound jet consisting of concentrically coflowing liquids (Figure 1).

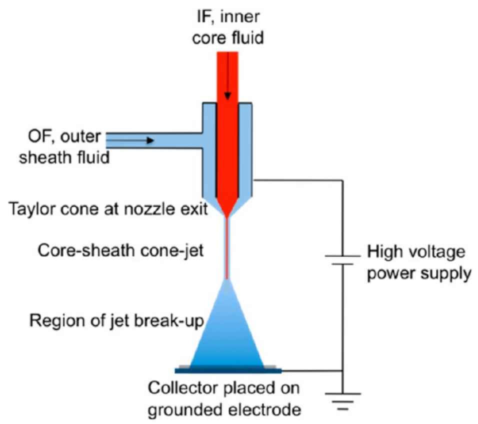

Figure 1. A schematic example of a coaxial EHD setup.

The charge distribution in a coaxial jet is dependent on the properties of the core and sheath liquids. To form a cone shape as a compound droplet at the capillary exit, at least one of the two liquids should enable a sufficient flow of charge. As the electrical relaxation time of a liquid is significantly faster than the viscous relaxation time in EHD processes,[21] charge is localized between the surface of the dielectric medium and the conducting liquid (also called the driving liquid).[21,22] In a typical single axial EHD process, this is localized at the interface between air and the charged liquid forming the Taylor cone. In a coaxial setup, if the electrical relaxation time of the sheath liquid is smaller than (or comparable to) that of the core liquid, charges are localized at the outer interface between the sheath and the air, and the sheath liquid is the driving liquid. On the other hand, the core liquid can also act as a driving liquid if the outer is a dielectric. In this case, when the driving interface is the innermost, the motion of the core liquid transmits to both the core and the sheath liquids via viscous forces, setting the compound liquid in motion to form a coaxial jet.[20,22] The flow rate of the driving liquid strongly affects the range of applied voltages that maintain the cone-jet mode[9] and in turn determines the reproducibility of the core–shell encapsulation, which requires simultaneous and concentric breakup of the compound jet.

Comprehensive theoretical and experimental research on coaxial electrospray have been discussed in the literature.[1,21,22] The materials and operating parameters that influence the formation of a stable coaxial Taylor cone at the capillary exit are also well studied.[21,23,24] When the outermost sheath polymer solution has sufficient viscoelasticity, fibers with an encapsulated core are produced instead of core–shell particles.[20] This process is also called coelectrospinning or coaxial electrospinning.[25] Hard-to-electrospin solutions or metal salts can be made into fibrous shape by coelectrospinning with a readily spinnable polymer serving as a template sheath for the core.[25−27] The carrier polymer may require removal at a later stage.

The addition of a carrier polymer increases the viscoelasticity of the spinning solution by increasing the degree of molecular entanglement in the liquid during uniaxial extensional flow.[11,12] Different from coelectrospinning, this work demonstrates that without using a carrier polymer or increasing the polymer concentration the concentric infusion of a Newtonian solvent such as water in the core of an electrified coaxial jet can cause the sheath polymer solution to electrospin instead of electrospray at a viscosity below 20 mPa s. Changing the core liquid from water to other Newtonian solvents with a range of different properties, such as DMF, ethanol, acetone, and glycerol, generated either beaded fibers or continuous fibers from the low-viscosity sheath solution, indicating that the process was not limited to one system. Key properties of the core solvent enabling continuous fiber formation rather than beaded fibers were studied. Core–shell solvent pairing, an important consideration in the formulation of multiaxial EHD coflow processes,[28] is discussed. Moreover, conventional EHD parameters such as flow rate and applied voltage control the degree of suppression of Rayleigh instability in the process and directly influence the final beaded or continuous fiber morphology. This work reports a new role of solvents in coaxial EHD techniques and presents a template-free method to generate micro- and nanofibers from low-viscosity polymer solutions without using carrier polymers. We also demonstrate that the process is applicable to other polymers of various molecular conformations, such as polycaprolactone (PCL) and polymethylsilsesquioxane (PMSQ).

2. MATERIALS AND METHODS

2.1. Materials. Poly(lactide-*co*-glycolide) (PLGA) copolymer 50:50, Resomer RG503H, number-average molecular weight (M_n) = 15 755 g mol^{-1}, was obtained from Boehringer Ingelheim (Ingelheim, Germany). Acetone, dimethyl carbonate (DMC), *N*,*N*-dimethylformamide (DMF), ethanol (EtOH), glycerol, and poly(ε-caprolactone) (PCL, M_n = 104 518 g mol^{-1}) were obtained from Sigma-Aldrich, Poole, UK. Polymethylsilsesquioxane (PMSQ, M_n = 1190 g mol^{-1}) was obtained from Wacker Chemie AG. All solvents obtained were of analytical grade. All materials were used as received.

PLGA and PCL are both flexible, long-chain, biocompatible polymers with important applications in biomedical and tissue engineering.[29,30] Under physiological conditions, amorphous PLGA and semicrystalline PCL bioerode at different degradation rates by hydrolysis to form nontoxic water-soluble monomers. PMSQ is a short-chain biocompatible polymer with a double-chain ladder-like structure. Pyrolysis of PMSQ yields ceramic silicon oxycarbide with applications in electronics, high-temperature structural reinforcements, and biomedical and optical materials due to attractive properties such as biocompatibility, high thermal and chemical durability, low

dx.doi.org/10.1021/ma5016616 | *Macromolecules* 2014, 47, 7930−7938

dielectric constant, antireflection, low density, and high mechanical strength.[31−33]

The polymer was mixed with the solvent at an appropriate ratio, and the mixture was mechanically stirred for 24 h to obtain a homogeneous solution. The main sheath solution used was PLGA in DMC, a solvent low in toxicity (VOC-exempt in the US) and rapidly biodegradable.[34] DMC was exempted under the definition of volatile organic compounds by the American Environmental Protection Agency in 2009.[35] DMC has a solubility profile similar to common glycol ethers, with an ester or alcohol-like odor. The Hildebrand solubility parameter of DMC is 20.3 MPa$^{1/2}$, and the Hansen solubility parameters are dispersion = 15.5 MPa$^{1/2}$, polar = 3.9 MPa$^{1/2}$, and H bonding = 9.7 MPa$^{1/2}$.[36]

2.2. Liquid Characterization. The density, viscosity, surface tension, and electrical conductivity of liquids were characterized under ambient conditions at 1 atmospheric pressure and 22−28 °C. Density was calculated by measuring the mass of the liquid in a 25 mL specific gravity bottle (VWR International, Lutterworth, UK) using an electronic balance (AND HF-1200G A&D Instruments Ltd., Japan). Viscosity was measured using LVDV III Ultra rheometer (Brookfield viscometers Ltd., UK). Surface tension was measured using the Wilhelmy's plate method (Kruss Tensiometer K9). Electrical conductivity was assessed using an HI-8733 (Hanna Instruments) conductivity probe. Distilled water was used for instrument calibrations. The instrument was cleaned with acetone and dried before each measurement. Data were calculated by averaging five measurements.

2.3. Electrohydrodynamic Processing. Figure 1 shows a schematic diagram of the coaxial EHD setup. Two liquids denoted by red and blue respectively, for the core liquid and the sheath liquid in the diagram were infused at appropriate flow rates through two concentrically assembled, stainless steel nozzles (stainless steel tubing, Stanley Engineering Ltd., Birmingham, UK). The core nozzle had an inner diameter (i.d.) of 0.686 mm and an outer diameter (o.d.) of 1.10 mm. The sheath nozzle had an i.d. of 2.03 mm and an o.d. of 2.60 mm. The dimensions of the nozzles influenced the initial droplet size at the nozzle exit. The o.d. of the core nozzle also set limits to the cross section of the sheath nozzle. The sheath nozzle was connected to the positive electrode of a high-voltage power supply (Glassman Europe Limited, Bramley, UK), which generated a dc applied voltage of up to 30 kV, relative to a stainless steel ground electrode kept at a distance of 50 mm. The core nozzle was not directly connected to a high voltage source. Hence, the electrical potential of the core liquid was dependent on the conductivity of the sheath liquid that was in direct contact with the charged outer sheath needle, which varied between that of the sheath nozzle and that of the ground electrode. The electrode connection in an EHD setup affects the charge transfer and distribution in a compound jet. Studies have varied the connection of the voltage supply, such as connecting to each of the coflowing liquids or to the outermost conductive nozzle.[22,37] These variations played a role in how charges were directly or sequentially transferred to core/sheath or all of the coflowing fluids simultaneously, which in turn affected the driving liquid. Connection of the electrode to the liquids in EHD processes should be clearly specified or standardized.

The outer sheath fluid (OF) was a polymer solution and the inner core fluid (IF) was a selection of solvents. The flow rates of the OF and IF were separately controlled by Harvard syringe pumps (Harvard Apparatus Ltd., Edenbridge, UK). The electric potential and flow rates of the fluids were varied to control the jetting modes and achieve steady cone-jet condition.[9,10] Particles or fibers were collected on glass slides covering the ground electrode for characterisation by optical and scanning electron microscopy. All processes were conducted and repeated under ambient conditions of 22−28 °C and 38−55% relative humidity.

2.4. Morphology Characterization. The morphology of the products was analyzed with a Nikon Eclipse ME600 optical microscope, a Hitachi S-3400N scanning electron microscope (SEM), and a field emission JSM-6301F SEM. Each SEM sample was coated with gold using a sputtering machine (Edwards sputter coater S 1 50B) for 60 s prior to observation. The micrographs were analyzed using Image Tool (UTHSCSA, Image Tool Version 2, University of Texas). Average diameters of the samples were determined from a minimum of 50 measurements.

3. RESULTS AND DISCUSSION

3.1. Core-Liquid-Induced Electrospinning of Low-Viscosity Poly(lactide-*co*-glycolide) Sheath Solution. Using a coaxial EHD setup, we report for the first time that without increasing the polymer concentration and without needing a template polymer, a sheath polymer solution at 17 mPa s can electrospin instead of electrospray in a coaxial electrified jet upon the infusion of a core liquid (Figure 2a,b).

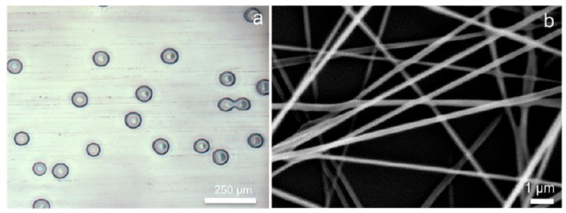

Figure 2. Electrified sheath-PLGA polymer solution with a viscosity of 17 mPa s, changed from (a) electrospraying particles in the absence of a core liquid to (b) electrospinning fibers (average diameter of 170 ± 50 nm) when water was infused in the core nozzle at 10 μL/min during coaxial electrohydrodynamic processing. Sheath flow rate was 50 μL/min, and the applied voltage was 11.5 kV for (a) and 15 kV for (b) over a collection distance of 50 mm.

Different from coelectrospinning, the core liquid can be a common solvent such as water and does not require a readily electrospinnable carrier polymer.[27,37] Without the presence of water as the core liquid, the sheath PLGA solution electrosprayed to form particles under all EHD operating conditions (Figure 2a).

Rayleigh−Plateau instability, driven by the surface tension of the solution, is responsible for particle electrospray instead of fiber electrospinning. The viscoelasticity of the polymer solution competes with Rayleigh instability and is conventionally determined by the polymer concentration or molecular weight. The relationship between viscoelasticity and the degree of molecular entanglement as a function of the critical overlap concentration in a polymer solution has long been established.[14,38] Increasing the polymer concentration or the entanglements in the solution causes particle electrospray to transit to fiber electrospinning, with beads-on-strings morphologies as a result of the incomplete suppression of Rayleigh instabilities. However, the presence of sufficient entanglement is not essential for fiber formation by electrospinning. Yu et al. distinguished the effect of elasticity versus that of viscosity and showed that if the relaxation time of an elastic liquid becomes longer than the growth rate of Rayleigh instabilities, electrospun fibers can form at low polymer concentrations with no entanglement transition and at shear viscosities less than 300 mPa s.[11] The relaxation time is defined as the characteristic time scale of the growth of elastic stress in uniaxial elongational flow. Figure 2 demonstrates that the infusion of water in the core of the PLGA solution caused the relaxation time of the compound jet to become longer than that of the pure PLGA solution as a single EHD jet. Depending on the core liquid and EHD operating conditions, the Rayleigh instability in the compound jet was suppressed to varying degrees leading to beaded or continuous fiber morphologies. This work examines the key parameters of this phenomenon.

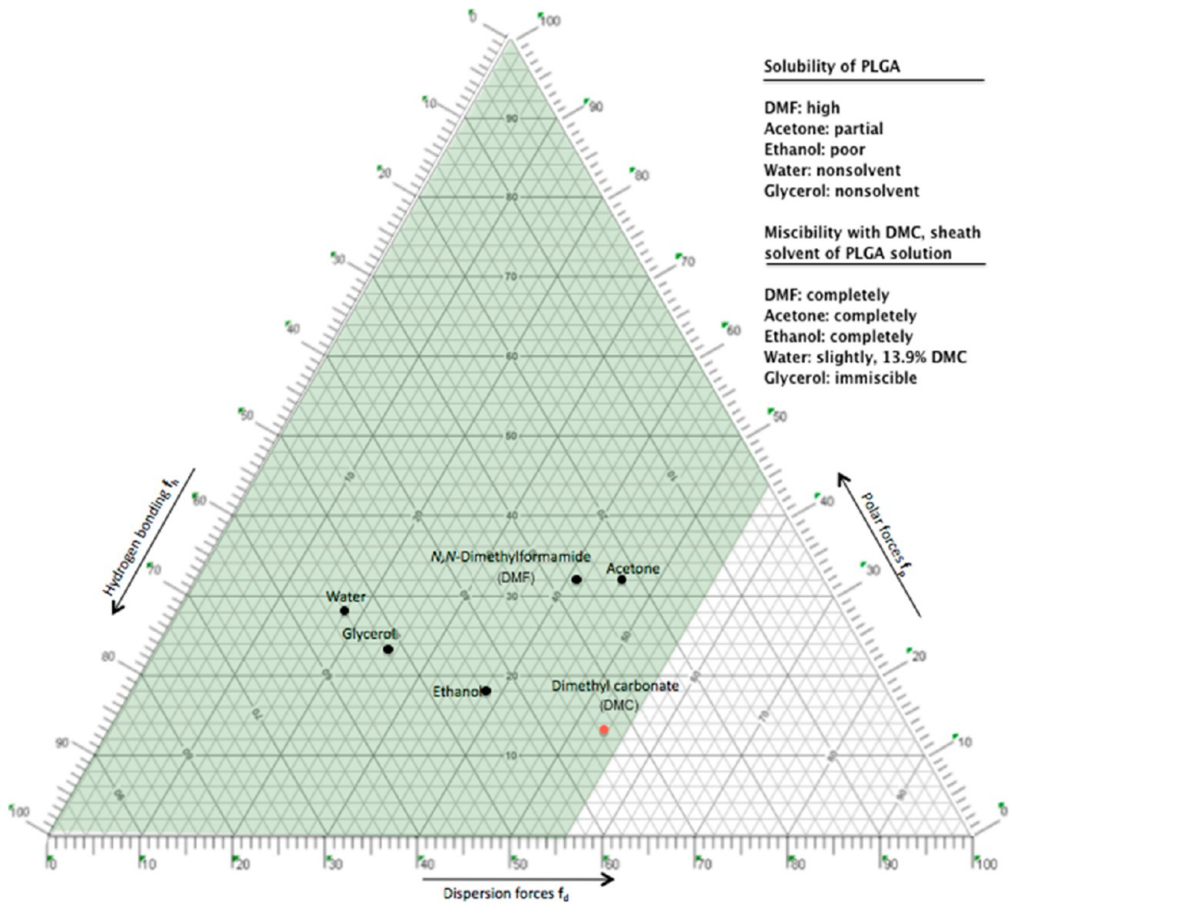

Figure 3. Solvents located on the Teas map. Black dots indicate selected core-nozzle liquids. Red dot represents the polymer solvent in the sheath liquid. Highlighted in green are regions of predominantly polar solvents. Solvents located in the polar region of the solvent map are selected to facilitate EHD processing and charge transfer in the compound liquid under an electric field.

Table 1. Liquid Properties[a]

sample	electrical relaxation time t_e (s) = $\varepsilon\varepsilon_0/\kappa$	electrical conductivity κ (S/m)	dielectric constant ε	viscosity η (mPa s)	density ρ (g/mL)	surface tension γ (mN/m)	$\gamma_{sheath} - \gamma_{core}$ (mN/m)	miscibility in DMC (25 °C)	solubility of PLGA
distilled water	5.9×10^{-6}	1.2×10^{-4}	79.7	0.89	1	72.75	−37.75	slightly, 13.9 g of DMC in 100 g of water[34]	no
glycerol	6.3×10^{-5}	6.0×10^{-6}	42.5	1499	1.26	63.3	−28.3	no	no
ethanol	1.4×10^{-3}	1.4×10^{-7}	22.4	1.08	0.789	22.3	12.7	yes	poor
DMC	1.4×10^{-4}	2.0×10^{-7}	3.1	0.664	1.07	31	4	yes	high
acetone	1.1×10^{-4}	5.0×10^{-7}	6.2	1.13	0.790	27.4	7.6	yes	partial
DMF	5.4×10^{-5}	6.0×10^{-6}	36.7	0.82	0.945	35	0	yes	high
17% w/w PLGA in DMC	2.7×10^{-4} [b]	1.0×10^{-7}		17	1.1	35			

[a]Properties of the PLGA solution and the electrical conductivity of DMC were experimentally determined due to lack of reported values. The electrical relaxation time, t_e, was calculated according to ref 21, where the vacuum permittivity $\varepsilon_0 = 8.85 \times 10^{-12}$ C^2 N^{-1} m^{-2}. Other data were cited from refs 34, 44, and 45. [b]Estimated using ε of DMC.

3.2. Solvent Properties. Infusing solvents with different properties (Figure 3 and Table 1) in the core generated either beaded fibers or continuous fibers from the sheath solution, demonstrating that the process was not limited to one system (Figure 4). We investigated key properties of the core solvent enabling continuous fiber formation rather than beaded fibers. The Teas map was used to visually present solvents based on the strengths of the three major intermolecular interactions, namely the dispersion forces, polar forces, and hydrogen bonding. The closer the solubility parameters of two solvents, the closer they were located on the map with similar range of intermolecular forces.[39,40]

When no core liquid was infused and when the core liquid and the sheath polymer solution had the same solvent (DMC) electrosprayed droplets formed due to classical Rayleigh–Plateau instability.[41,42] No transition from electrospray to electrospinning was observed under any EHD conditions, and encapsulation as compound droplets was readily obtained (Figure 4a,b). This result concurred with previous published work showing that the same solvent for both coflowing polymer

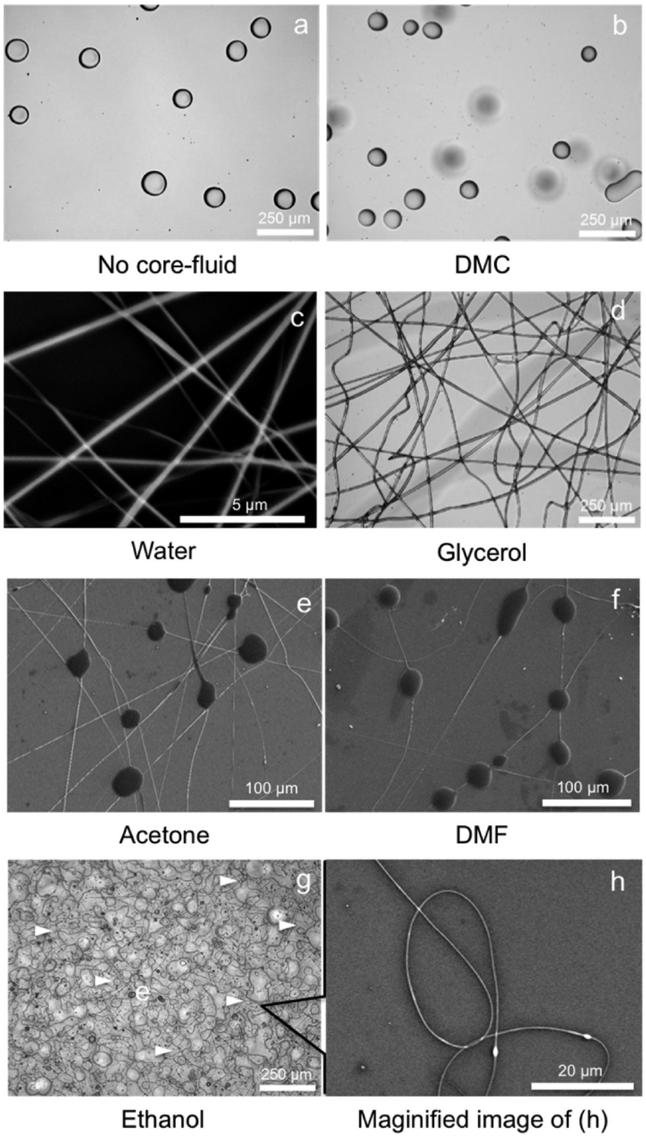

Figure 4. A range of core solvents of different properties in coaxial flow under an EHD process can cause a low-viscosity sheath PLGA solution (17 mPa s) to form fibers. Core liquids are (a) empty core nozzle, (b) DMC, (c) water, (d) glycerol, (e) acetone, (f) DMF, (g, h) ethanol; (h) is a higher magnification image of (g) showing the presence of fibers between the merged droplets observed in (g). White arrows highlight the fibers. Droplets merged in ethanol, which was a poor solvent of PLGA. Steady cone jet was not achieved when ethanol was infused as the core liquid.

solutions readily generated compound droplets in coaxial electrospray.[24,43]

It is well-known that mixing the same solvent to a polymer solution only dilutes the solution, whereas a polymer coil would contract when a poorer solvent was mixed in a polymer dissolved in a good solvent.[46] Our previous work using the Teas solvent map also showed that poorer solvents can reduce the critical solution concentration required for electrospinning.[39] The difference in solubility for PLGA between the core and sheath solvents was studied in section 3.2.1 for the influence on the molecular behavior of the polymer at the interface upon contact with a poorer solvent and the subsequent effect on the process. Moreover, solubility and miscibility were considered together as solvent mixtures were involved. For example, water is a nonsolvent of PLGA. DMC is only slightly miscible with water. A maximum of 13.9 g of DMC can be dissolved in a 100 mL of water.[34] In practice, the low miscibility resulted in relatively slow diffusion between DMC and water. In practice, no coagulation was observed at the core−sheath interface in the compound droplet.

3.2.1. Effect of Solubility and Miscibility. The process occurred irrespective of the solubility or miscibility of the core and sheath liquids (Figures 3 and 4), though in the case of a nonsolvent, low miscibility may be preferred to ensure that the polymer solution does not precipitate quickly at the core−sheath interface. DMF, acetone, and ethanol are completely miscible with sheath solution. Glycerol and water are, respectively, immiscible and poorly miscible with DMC. The solubility of the above solvents for PLGA is DMF (good solvent) > acetone (partial solvent) > ethanol (poor solvent) > water (nonsolvent) and glycerol (nonsolvent) (for details on how degree of solubility was defined, see ref 40). It was noted that solvents close to each other on the map generated similar fiber morphologies. For example, both glycerol and water caused fibers with few or no beads (Figures 3 and 4c,d), and both acetone and DMF caused beaded fibers of similar morphology (Figures 3 and 4e,f).

The stability of the core−sheath liquid interface as the core solvent of a different solubility comes into contact with the sheath solution was investigated and correlated with the process. The interface between the core and sheath solution inside the compound droplet exiting the coaxial nozzle was hard to image. Hence, we observed using optical microscopy a droplet of the PLGA sheath solution coming into contact with a droplet of a solvent on a glass slide. A visible motion or "shrinkage" of the PLGA solution at the liquid−solution interface was observed with poor or nonsolvents, a macroscopic behavior that indicated polymer coil contraction at the interface due to reduced solubility. The "shrinkage" at the interface was qualitatively observed as instantaneous and strong for glycerol and water, two nonsolvents; to a lesser but clearly visible degree for ethanol and acetone, two poor/partial solvents; and no visible shrinkage was observed for DMC (same solvent) and DMF (good solvent). Together with Figure 4, this observation shows that though a different solvent of lower solubility can cause instability at the core−shell liquid interface, poorer solubility was not a determining factor in the process, as good solvents such as DMF also caused fiber formation.

3.2.2. Effect of Surface Tension, Electrical Conductivity, and Dielectric Constant. In addition to miscibility and solubility, the surface tension of the core liquid was a key parameter in the process, compared to other important EHD material parameters including electrical conductivity and dielectric constant. In a coaxial EHD flow, the surface charge due to the electric field induces a motion in the sheath polymer solution, causing shear at the core−sheath interface. The formation of a steady compound cone jet was affected by the conductivity, the dielectric constant, and the core and sheath surface tension of the liquids.[1,6] The solvents in Table 1 exemplified a broad range of the aforementioned properties. To study the influence of liquid properties on compound cone-jet stability, we also imaged the shape of the jet at the nozzle exit during the induced fiber formation by various core liquids (Supporting Information Figure S1; for classifications of EHD jetting modes and various shapes of the jet at the nozzle exit, see ref 10).

The results suggested that high surface tension of the core liquid and high interfacial tension between the core and the sheath liquids strongly influenced the fiber-forming process; differences in dielectric constant and electrical conductivity of the liquids did not significantly affect fiber formation. For example, DMF and glycerol have comparable electrical conductivity and dielectric constant but differ significantly in surface tension (Table 1). DMF caused beaded fibers whereas glycerol generated continuous fibers (Figure 4d,f). Furthermore, DMF and acetone had different dielectric constant values but were comparable in the range of surface tension and electrical conductivity (Table 1). The morphology of the fibers caused by DMF and acetone were similar (Figure 4e,f). In addition, we calculated the electrical relaxation time t_e, a parameter that correlated the electrical conductivity and dielectric constant. t_e is the time required to smooth a perturbation in an electric charge and is given by $\varepsilon\varepsilon_0/\kappa$, where ε_0 is the vacuum permittivity and ε and κ are respectively the dielectric constant and electrical conductivity of the liquid (Table 1).[21] Although glycerol and water have higher values of dielectric constant in comparison with all the solvents tested (Table 1), t_e of glycerol at 6.3×10^{-5} s was not significantly different from that of DMF (5.4×10^{-5} s). Taking together the analyses on solvent properties, the key core liquid parameter in the process was high surface tension.

3.3. Influence of EHD Operating Parameters. An electrified liquid jet in an EHD process experiences competing instabilities including the Rayleigh−Plateau instability, the axisymmetric conducting instability, and the whipping instability (bending instability).[41,42] These competing instabilities exist in both electrospray and electrospinning processes, and the whipping instability can occur in the absence of viscoelasticity,[11] as exemplified in an electrified water jet.[47] The instability dominating the electrified jet as it accelerates from the nozzle exit toward the ground electrode depends on both the material properties of the liquid and the operating parameters of the process, such as flow rates and applied voltages. Using water as the core liquid, the core and sheath flow rates and the electrical potential were varied, and the resultant polymer structures were studied under optical and scanning electron microscopy to further elucidate the process. The operating conditions are listed in Table 2.

While keeping all other parameters constant, increasing the voltage from 9.5 kV (Figure 5a) to 11.5 kV (Figure 5b) resulted in a bimodal distribution of droplet size under a steady jet. The larger particles were 103 ± 18 μm in diameter; the satellite particles were 5.1 ± 1.3 μm in diameter.

Table 2. EHD Operating Parameters for Results Presented in Figures 5−7

Figure	core flow rate (μL/min)	sheath flow rate (μL/min)	applied voltage (kV) at 50 mm electrode distance
5a	0	150	9.5
5b	0	150	11.5
5c	0.5	150	11.5
6a	10	150	13.5
6b	10	100	13.5
6c	10	50	15.0
7a	10	50	15.0
7b	20	50	15.0
7c	30	50	15.0

While both Figures 5a,b were obtained in the absence of a core liquid, Figure 5c was obtained under the same applied voltage and sheath flow rate of Figure 5b, but with water infused at 0.5 μL/min in the core nozzle. The same bimodal particle distribution was observed, though the second-generation satellite droplets formed beads-on-strings (Figure 5c). This beads-on-string formation has been well documented in unentangled viscoelastic single liquids as the growth rate of the Rayleigh instability competes with the relaxation time of the liquid.[11,16] The presence of water in the compound jet is believed to increase the relaxation of the sheath liquid. To quantify this relationship, further studies should characterize the extensional properties of the compound jet such as the Deborah number and the critical value of elastic stress in the compound jet at various core−sheath flow rates.[11] Increasing the infusion rate of the core liquid water further to 10 μL/min (Figure 6a) caused a steady jet generating beads-on-string fibers at 13.5 kV. The diameter and frequency of the beads on the fibers reduced as the flow rate of the PLGA solution reduced from 150 μL/min (Figure 6a) to 100 μL/min (Figure 6b) and to 50 μL/min (Figure 6c).

The same process of fiber formation, detailed in Figures 5 and 6, was observed when infusing other liquids in the core. Supporting Information Figure S2 demonstrates the process using glycerol in the core for parallel comparison with Figures 5 and 6; the sheath PLGA solution changed from producing spherical particles (Figure S2a), to smaller particles with tapered "tails" (Figure S2b,c), to beaded fibers (Figure S2d), and to continuous bead-free fibers (Figure S2e). Prior to forming fibers due to the infusion of a core liquid, satellite droplets of various patterns were often observed. When the core liquid was water or glycerol, the satellite droplets aligned in a linear fashion before fiber generation (Figure 5c and Figure S3a), whereas when using DMF, the satellite droplets aligned in a circular fashion prior to forming beaded fibers (Figure S3b). Similar to when water was tested as the core liquid, the flow rate of the core and sheath liquids affected the process when using other liquids in the core nozzle.

The electric field strength required for a steady cone jet varied with the flow rate of the liquids (Table 2), though cone jet was achievable under a range of flow rates and voltages, as discussed in detail in our earlier work.[8] To obtain a structured Taylor cone, the electrical forces must act on at least one liquid, although they may act on both. The driving liquid is the liquid upon which the electrical forces act to form the Taylor cone.[22] The flow rate of the driving liquid/compound liquids determines the range of applied voltage to form a steady cone jet in coaxial EHD.[21,22] In this study, charge was first transferred to the sheath PLGA solution, but the distilled water infused in the core had a lower electrical relaxation time than the sheath solution (Table 1). Hence, the electrical forces acted on both liquids, and the flow rates of the sheath and the core liquids affected the cone-jet voltage (Table 2).

Oguz and Sadhal[48] analyzed compound multiphase droplets of two immiscible liquids and showed that the applied electric field affected the motion of the core liquid with respect to the sheath liquid. Fiber formation from the sheath polymer solution became more abundant with increasing electric force on the compound jet, as the applied voltage increased from 13.5 and 18.7 kV (Figure S4), while keeping other parameters the same as that for Figure 6a. However, the cone jet became unstable at above 20 kV, as conditions approached the dielectric

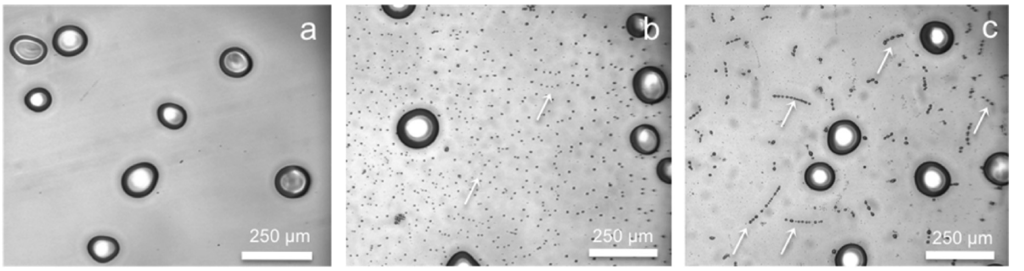

Figure 5. Optical micrographs showing PLGA particles produced at sheath-solution flow rate of 150 μL/min under a steady cone jet: (a) first-generation particles formed with an empty core nozzle, voltage at 9.5 kV; (b) first-generation particles with second-generation satellite particles formed with an empty core nozzle, voltage at 11.5 kV. White arrows indicate the satellite droplets. (c) "Beads-on-string" filaments arising from incomplete breakup of second-generation satellite particles when water was infused at 0.5 μL/min; all other parameters were the same as (b).

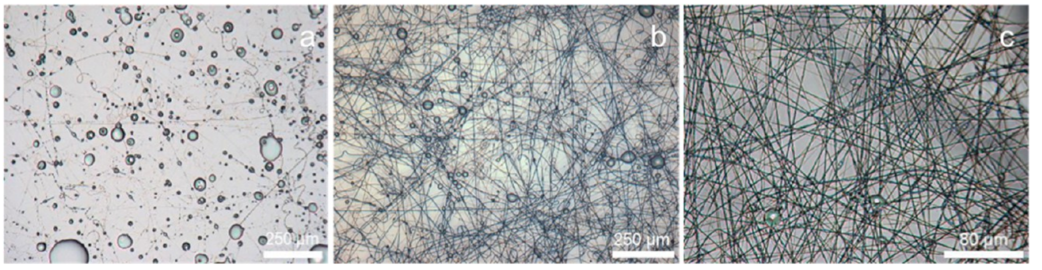

Figure 6. Optical micrographs showing increasing fiber formation when sheath PLGA solution flow rate was varied, while water was infused through the core nozzle at 10 μL/min: (a) 150, (b) 100, and (c) 50 μL/min.

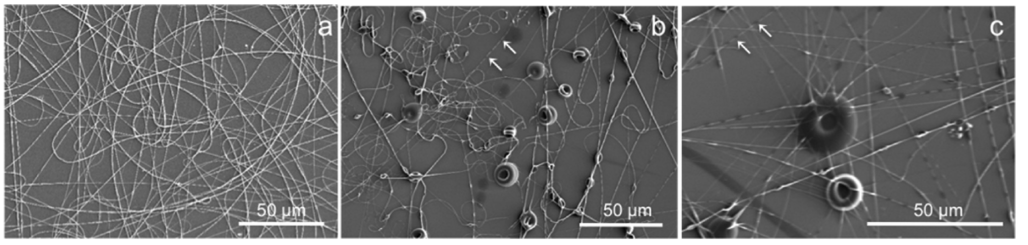

Figure 7. Influence of core-liquid flow rate on the transition between electrospray and electrospinning of sheath PLGA solution. Water was infused at (a) 10, (b) 20, and (c) 30 μL/min. White arrows highlight darker shades on the fibers in (b) and (c) indicating an encapsulated core.

breakdown of the ambient air. Large beads were observed at 20.2 kV.

In addition, the flow rate of the core liquid influenced the process. The resulted polymer structure changed as the core liquid changed from absent (Figures 5b) to being infused at 0.5 and 10 μL/min (Figure 5c and 6a). Moreover, at a sheath PLGA solution flow rate of 50 μL/min, when water flow rate further varied between 10, 20, and 30 μL/min, the resultant fiber morphology changed from near-continuous fibers (Figures 7a) to necklace-like, large bead-on-string fibers (Figure 7b,c). The beads formed on the bead-on-string fibers at higher water flow rate of 20−30 μL/min were different in size (10−20 μm) from the satellite particles of 5.1 ± 1.3 μm, which were observed prior to the transition to electrospinning (Figure 5c).

At a constant flow rate of PLGA and a constant applied voltage, the increased flow rate of water from 10 to 30 μL/min reduced the charge density of the compound liquid. The reduced charge density led to the surface tension of water in the compound jet to overcome the electrical force that elongated the jet, forming beaded fibers, with water in the fiber core, shown as the darker shades on the fibers (white arrows in Figure 7b,c). The darker shades on the fibers were similar to the beads-on-fiber morphology reported in coelectrospinning.[20] Further fiber characterization is required to investigate if the internal structure of the fibers were hollow or porous as the core solvent leaves the fibers. Fluorescent markers/dyes may be added to more clearly visualize the deposition of the core/shell liquids during fiber formation.

3.4. Relevance to Other Polymer Systems. The process reported in this work was not limited to PLGA polymer (M_n = 15 755 g mol^{-1}). We demonstrated the same effect using another polymer with a higher molecular weight, polycaprolactone (PCL, M_n = 104 518 g mol^{-1}), and a macromolecule with a lower molecular weight, polymethylsilsesquioxane (PMSQ, M_n = 1190 g mol^{-1}). Water was used as the core liquid to illustrate both cases. Figure S5a shows electrosprayed beads from 7% w/w PCL solution in acetic acid in the absence of a core liquid. When water was infused in the core nozzle at 10 μL/min, the sheath−PCL solution produced beaded fibers (Figure S5b). The bead diameter reduced from 120 μm during electrospray (Figure S5a) to below 10 μm on the bead-on-string fibers (Figure S5b). In addition, PMSQ with a ladder-like molecular conformation was used. Samples of PMSQ at the low M_n of 1190 g mol^{-1} can only electrospray under conventional EHD conditions. Figure S5c,d shows 50% w/w PMSQ in ethanol solutions forming beaded microfibers when water was infused at 10 and 20 μL/min (Figure S5c,d).

As discussed earlier in section 3.2, the process occurred irrespective of the core−sheath liquid miscibility. In addition, both solvents and nonsolvents infused in the core could cause sheath-fiber formation, though a miscible nonsolvent was not desirable for the process. For example, water was a nonsolvent of PCL and PMSQ and was completely miscible with acetic acid and ethanol—the respective sheath solvents. Water allowed the process to occur, though the EHD process eventually came to a halt as the high miscibility between the nonsolvent and the sheath solution gradually precipitated the polymer at the core−sheath interface. These examples also reinforced our earlier discussion that immiscibility or poor miscibility between the core and the sheath liquids would be desirable if a nonsolvent was used as the core liquid in the process.

4. CONCLUSIONS

This work reports for the first time that the core liquid in an electrified coaxial jet can cause an electrospraying low-viscosity (<20 mPa s) sheath polymer solution to undergo fiber electrospinning without increasing the polymer concentration. The process does not require a sheath template polymer. The core liquid can be a common solvent such as water. The technique is not limited to one system; a variety of core liquids with different solvent properties can cause fiber electrospinning. These include water, glycerol, ethanol, acetone, and dimethylformamide, demonstrating that miscible, partially miscible, and immiscible solvents and nonsolvents of the sheath solution induce fiber formation to varying levels. The presence of core liquids contributes to the suppression of Rayleigh instability, leading to the transition from electrospray to electrospinning of beads-on-strings or continuous fibers. Key parameters in the process are high surface tension of the core solvent and high interfacial tension at the core−sheath interface as well as the operating flow rate and applied voltage. The dielectric constant and electrical conductivity of the core liquid are not significant factors influencing the process. We also demonstrate the process using a variety of polymers including PLGA, PCL, and PMSQ systems. Future work should characterize the internal structures of the fibers. This work documents new roles of solvents in an electrified coaxial jet and facilitates the effective fabrication of core−shell polymeric micro- and nanostructures by coaxial EHD processes. It also presents a potential method to obtain micro- and nanofibers from low-viscosity solutions without using a template polymer that may require removal at a later stage.

■ ASSOCIATED CONTENT

Ⓢ Supporting Information

Figures S1−S5. This material is available free of charge via the Internet at http://pubs.acs.org.

■ AUTHOR INFORMATION

Corresponding Author

*E-mail chaojie.luo@ucl.ac.uk, Tel +44(0) 20 76793920, Fax +44(0) 20 73880180 (C.J.L.).

Notes

The authors declare no competing financial interest.

■ ACKNOWLEDGMENTS

The authors thank EPSRC and a UCL Knowledge Transfer and Enterprise Award for supporting this work.

■ REFERENCES

(1) Barrero, A.; Loscertales, I. G. *Annu. Rev. Fluid Mech.* **2007**, *39*, 89−106.
(2) Carletti, E.; Motta, A.; Migliaresi, C. In *3D Cell Culture*; Haycock, J. W., Ed.; Methods in Molecular Biology; Humana Press: New York, 2011; pp 17−39.
(3) Anderson, D. G.; Burdick, J. A.; Langer, R. *Science* **2004**, *305*, 1923−1924.
(4) Luo, C. J.; Loh, S.; Stride, E.; Edirisinghe, M. *Food Bioprocess Technol.* **2012**, *5*, 2285−2300.
(5) Luo, C. J.; Stoyanov, S. D.; Stride, E.; Pelan, E.; Edirisinghe, M. *Chem. Soc. Rev.* **2012**, *41*, 4708−4735.
(6) Taylor, G. *Proc. R. Soc. London* **1964**, *280*, 383−397.
(7) Mestel, A. J. *J. Fluid Mech.* **1994**, *274*, 93−113.
(8) Ghanbar, H.; Luo, C. J.; Bakhshi, P.; Day, R.; Edirisinghe, M. *Mater. Sci. Eng., C* **2013**, *33*, 2488−2498.
(9) Cloupeau, M.; Prunetfoch, B. *J. Electrost.* **1989**, *22*, 135−159.
(10) Cloupeau, M.; Prunetfoch, B. *J. Electrost.* **1990**, *25*, 165−184.
(11) Yu, J. H.; Fridrikh, S. V.; Rutledge, G. C. *Polymer* **2006**, *47*, 4789−4797.
(12) Rutledge, G. C.; Fridrikh, S. V. *Adv. Drug Delivery Rev.* **2007**, *59*, 1384−1391.
(13) Fong, H.; Chun, I.; Reneker, D. H. *Polymer* **1999**, *40*, 4585−4592.
(14) Shenoy, S. L.; Bates, W. D.; Frisch, H. L.; Wnek, G. E. *Polymer* **2005**, *46*, 3372−3384.
(15) Collins, R. T.; Jones, J. J.; Harris, M. T.; Basaran, O. A. *Nat. Phys.* **2008**, *4*, 149−154.
(16) Oliveira, M. S. N.; McKinley, G. H. *Phys. Fluids* **2005**, *17*, 071704.
(17) Chang, M. -w.; Stride, E.; Edirisinghe, M. *J. R. Soc. Interface* **2010**, *7*, S377−S378.
(18) Ekemen, Z.; Chang, H.; Ahmad, Z.; Bayram, C.; Rong, Z.; Denkbas, E.; Stride, E.; Vadgama, P.; Edirisinghe, M. *Biomacromolecules* **2011**, *12*, 4291−4300.
(19) Li, D.; Xia, Y. N. *Nano Lett.* **2004**, *4*, 933−938.
(20) Diaz, J. E.; Barrero, A.; Marquez, M.; Loscertales, I. G. *Adv. Funct. Mater.* **2006**, *16*, 2110−2116.
(21) López-Herrera, J. M.; Barrero, A.; López, A.; Loscertales, I. G.; Márquez, M. *J. Aerosol Sci.* **2003**, *34*, 535−552.
(22) Loscertales, I. G.; Barrero, A.; Guerrero, I.; Cortijo, R.; Marquez, M.; Ganan-Calvo, A. M. *Science* **2002**, *295*, 1695−1698.
(23) Chen, X.; Jia, L.; Yin, X.; Cheng, J.; Lu, J. *Phys. Fluids* **2005**, *17*, 032101.
(24) Mei, F.; Chen, D. R. *Phys. Fluids* **2007**, *19*, 103303:1−10.
(25) Sun, Z. C.; Zussman, E.; Yarin, A. L.; Wendorff, J. H.; Greiner, A. *Adv. Mater.* **2003**, *15*, 1929−1932.
(26) Yarin, A. L.; Zussman, E.; Wendorff, J. H.; Greiner, A. *J. Mater. Chem.* **2007**, *17*, 2585−2599.
(27) Ojha, S. S.; Stevens, D. R.; Hoffman, T. J.; Stano, K.; Klossner, R.; Scott, M. C.; Krause, W.; Clarke, L. I.; Gorga, R. E. *Biomacromolecules* **2008**, *9*, 2523−2529.
(28) Labbaf, S.; Ghanbar, H.; Stride, E.; Edirisinghe, M. *Macromol. Rapid Commun.* **2014**, *35*, 618−623.
(29) Ratner, B.; Hoffman, A.; Schoen, F.; Lemons, J. *Biomaterials Science: An Introduction to Materials in Medicine*; Elsevier Academic Press: London, 2004.
(30) Jain, A. *Biomaterials* **2000**, *21*, 2475−2490.
(31) Ma, J.; Shi, L. H.; Shi, Y. Y.; Luo, S. U.; Xu, J. *J. Appl. Polym. Sci.* **2002**, *85*, 1077−1086.
(32) Zhuo, R.; Colombo, P.; Pantano, C.; Vogler, E. A. *Acta Biomater.* **2005**, *1*, 583−589.
(33) Colombo, P.; Riedel, R.; Sorarù, G. D.; Kleebe, H. J. *Polymer Derived Ceramics: From Nano-structure to Applications*; DEStech Publications, Inc.: Lancaster, PA, 2010.
(34) Tundo, P.; Selva, M. *Acc. Chem. Res.* **2002**, *35*, 706−716.
(35) Environmental Protection Agency (EPA). Air Quality: Revision to Definition of Volatile Organic Compounds-Exclusion of Propylene Carbonate and Dimethyl Carbonate, 3437−3441 [E9-1150] http://

regulations.justia.com/regulations/fedreg/2009/01/21/E9-1150.html (accessed July 25, 2014).
(36) Kowa American Corp. Dimethyl carbonate PP revison April; www.american-coatings-show.com. Last accessed 26 August 2012, 2009.
(37) Yarin, A. L.; Zussman, E.; Wendorff, J. H.; Greiner, A. *J. Mater. Chem.* **2007**, *17*, 2585−2599.
(38) McKee, M. G.; Elkins, C. L.; Long, T. E. *Polymer* **2004**, *45*, 8705−8715.
(39) Luo, C. J.; Nangrejo, M.; Edirisinghe, M. *Polymer* **2010**, *51*, 1654−1662.
(40) Luo, C. J.; Stride, E.; Edirisinghe, M. *Macromolecules* **2012**, *45*, 4669−4680.
(41) Shin, Y. M.; Hohman, M. M.; Brenner, M. P.; Rutledge, G. C. *Appl. Phys. Lett.* **2001**, *78*, 1149−1151.
(42) Hohman, M. M.; Shin, M.; Rutledge, G.; Brenner, M. P. *Phys. Fluids* **2001**, *13*, 2201−2220.
(43) Lee, Y. H.; Mei, F.; Bai, M. Y.; Zhao, S.; Chen, D. R. *J. Controlled Release* **2010**, *145*, 58−65.
(44) Smallwood, I. M. *Handbook of Organic Solvent Properties*; Arnold: London, 1996.
(45) Sevas Educational Society. *Properties of glycerine*; http://www.sbioinformatics.com/design_thesis/Glycerol/Glycerol_-2520Properties&uses.pdf. Last accessed 3 August, 2012.
(46) Graessley, W. W. *Adv. Polym. Sci.* **1974**, *16*, 1−179.
(47) Magarvey, R. H.; Outhouse, L. E. *J. Fluid Mech.* **1962**, *13*, 151−157.
(48) Oguz, H. N.; Sadhal, S. S. *Q. J. Mech. Appl. Math.* **1989**, *42*, 65.